

The effect of mixing and initial CCN concentrations on the condensational growth of droplets in clouds.



Alison Coals, Alan Gadian , Alan Blyth , Wojciech Grabowski⁽²⁾, Jean-Louis Brenguier⁽³⁾ and John Latham⁽²⁾

University of Leeds , NCAR⁽²⁾, CNRM⁽³⁾

Aims and Objectives

Project Aim:

The overall aim of the project was to understand the growth of the condensation droplet spectra in non-precipitating convective clouds.

Specific Objectives:

To use observations from cumulus clouds to analyse the growth of the droplet spectra; in this case using SCMS data

To use a simplified microphysical model parameterisation of activation, droplet growth to model mixing and entrainment in a 3-d cloud resolving model.

To understand the differences between the modelled and observed spectra, and using sensitivity studies to examine the role of turbulent mixing processes, to explain the differences in cloud spectra

Microphysical Approach:

Numerical simulations of cloud microphysical processes, especially for activation of (CCN) and droplet growth are computationally intensive. Brenguier and Grabowski (1993) developed Brenguier's (1991) b^2 approach, which used a much simplified and analytically integrable droplet growth equation.

This greatly reduced the computational overheads whilst at the same time representing both the CCN activation and droplet growth processes. Using a 3-dimensional CRM, model and observed condensational droplet distributions are contrasted. The difference in cloud droplet spectra in different regions of cloud is examined, as are the physical processes of entrainment and turbulent mixing. The condensational growth of cloud droplets are subject to inhomogeneous and homogeneous mixing and entrainment.

Numerical Model

The three-dimensional non-hydrostatic anelastic fluid model of Smolarkiewicz and Margolin (1997) is used to simulate observed clouds. The model incorporates the droplet microphysical scheme of Brenguier (1991), where the CCN activation process is parameterized, total droplet condensation in non-diluted cloud volume is assumed constant and equal to initial concentration N_0 . Following Brenguier and Grabowski (1993), a simplified form of the droplet condensational growth equation is used,

$$\frac{dr}{dt} = \frac{AS(t)}{r+a}$$

where a is the accommodation coefficient, A is a constant, and S is the supersaturation. When this is integrated along a path in a cloud gives

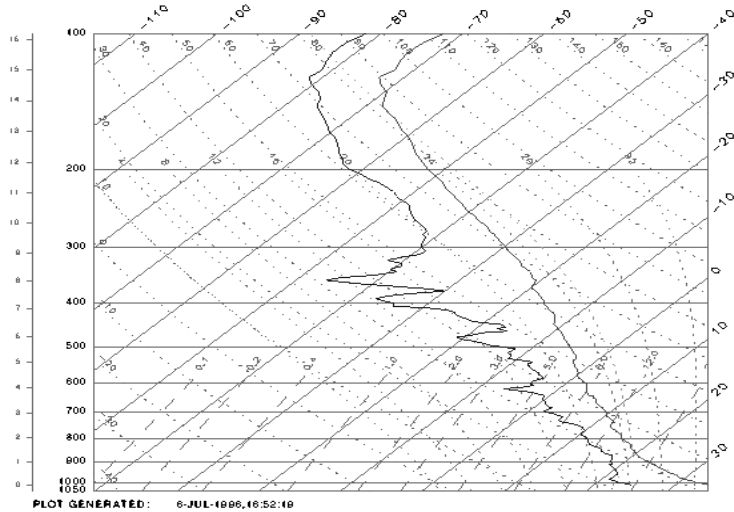
$$(r+a)^2 = (r_0+a)^2 + b^2(t),$$

where r_0 is the initial radius at initial time t_0 and

$$b^2(t) = (r+a)^2 - (r_0+a)^2 = 2A \int_{t_0}^t S(t) dt.$$

This parameter, b^2 , represents the summation of the supersaturation history of the parcels, which determines the growth of the spectrum.

SITE: FKED, IS4 TIME: 24-JUL-1995,18:38:00 (F7244835.IS4) TEMP/WINDS DEWPOINT

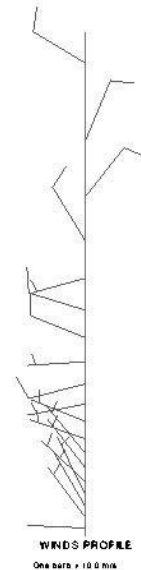
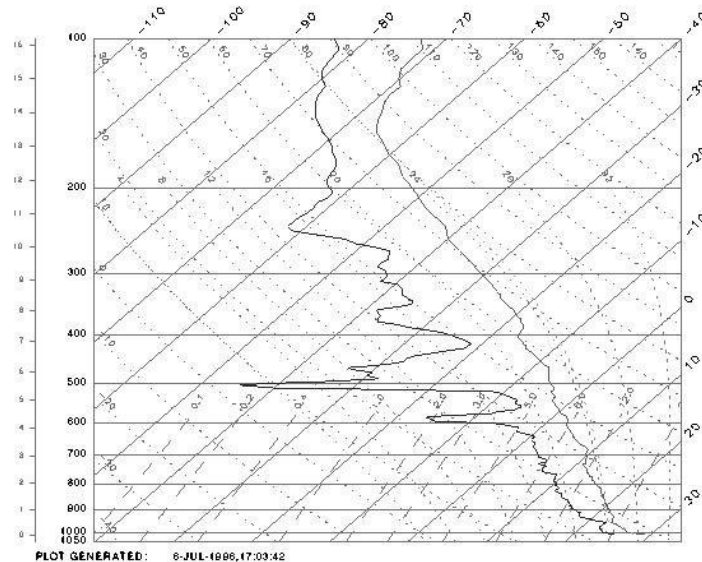


24/7/95 at 18:38 UTC
Droplet conc $\sim 800 \text{ cc}^{-1}$
“continental” type

Tephigrams used to
initialise the model,
taken $\sim 22\text{km}$ from site.

10/8/95 at 14:08 UTC
Droplet conc $\sim 530 \text{ cc}^{-1}$

SITE: FKED, IS4 TIME: 10-AUG-1995,14:08:20 (F8101408.IS4) TEMP/WINDS DEWPOINT



24th July 1995 SCMS case study of a
“continental” type cloud

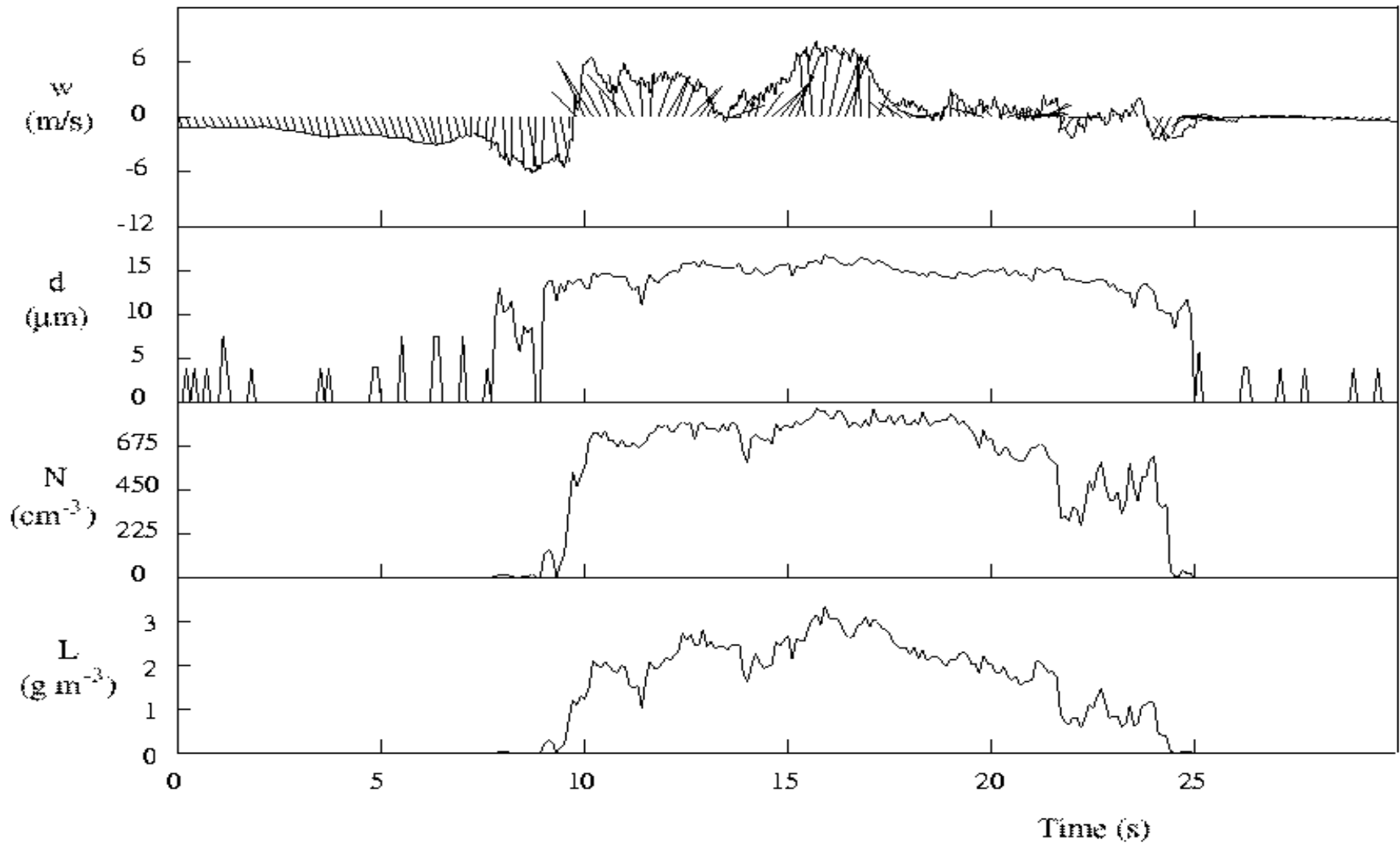


Fig 2. Time series of data gathered beginning at 1732:15. The top panel shows the 25 Hz vertical wind speed (w) superimposed with wind vectors calculated from the vertical wind and horizontal wind along the direction of motion; the bottom three panels are 10 Hz values of mean diameter, total concentration of cloud drops N , and liquid water content, L , respectively, derived from the FSSP. (24/7/ 95)

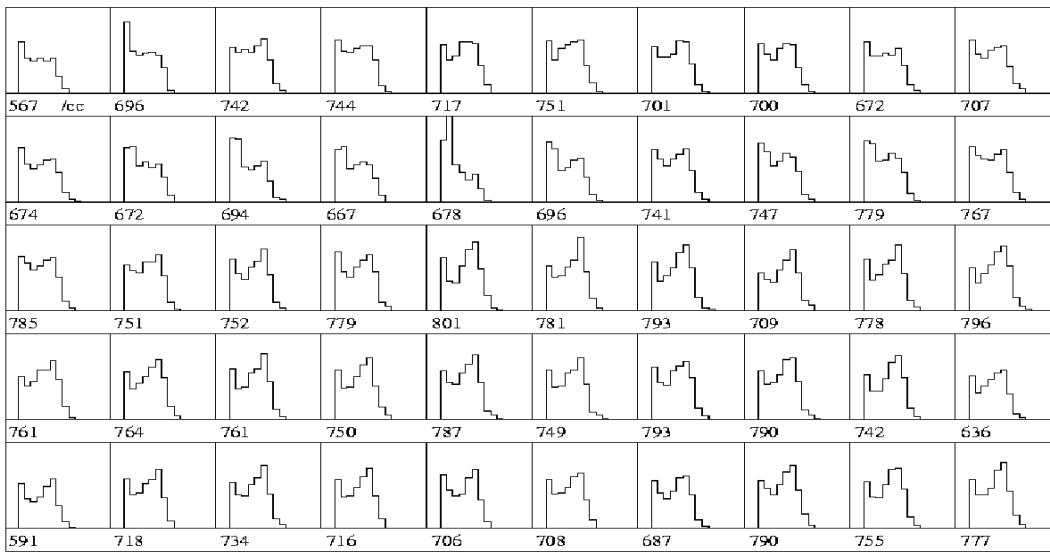


Fig.3 10 Hz drop size distributions measured by the FSSP, commencing at 1732:15 (top left) and ending at 1732:20 (bottom right). The x-axis is diameter ranging from 0 - 50 μm and the y-axis is $N(d)$, ranging from 0 - 200 cm^{-3} .

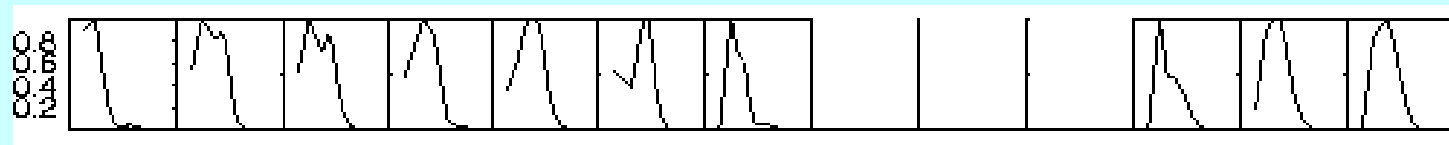


Fig. 4 Simulated drop size distributions through cloud along flight path (altitude 2.7 km), ($N_0=1000 \text{ cm}^{-3}$). Each plot represents a grid point in the model (95 m), and corresponds to approximately 1 second of flight time, from top left to bottom right. The x-axis is diameter ranging from 0--40 μm and the y-axis is the normalized distribution.

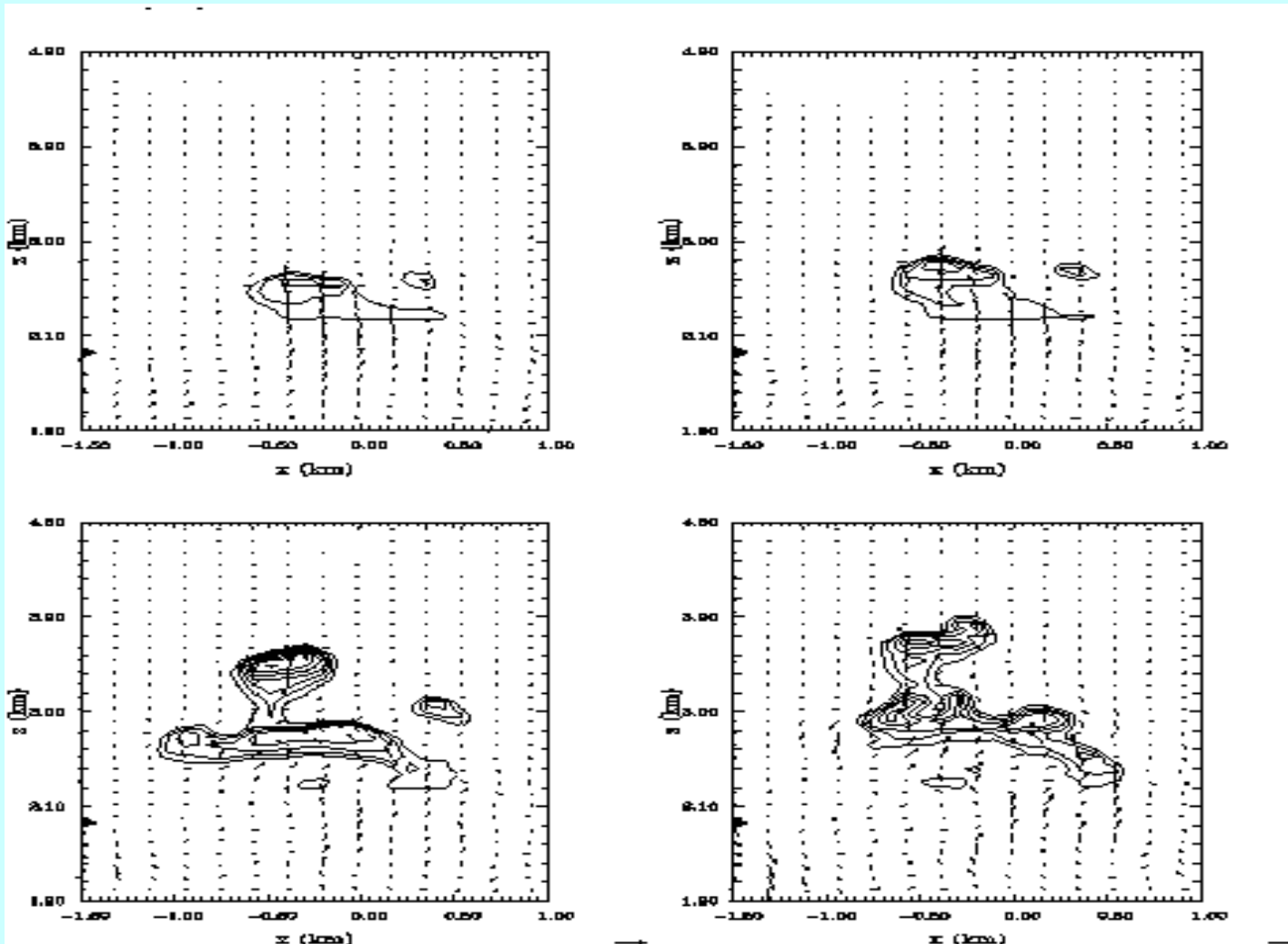


Fig 5. Vertical cross-sections of simulated cloud with wind vectors overlaid at (top left) 46, (top right) 48, (bottom left) 51, and (bottom right) 53 mins.

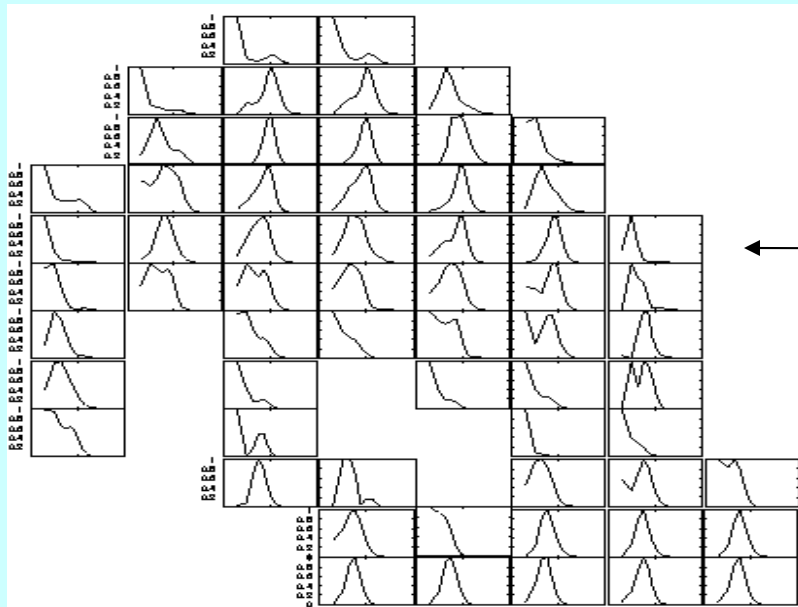


TABLE 1. 24TH JULY 1995: SIMULATED VERTICAL VELOCITIES AND CLOUD WATER MIXING RATIOS FOR THE UPPER REGION OF THE CLOUD AT 48 MINUTES.

Height (m)	Distance from edge of cloud (m)									
	0	95	190	285	380	475	570	665	760	
3144			5.14	5.11						
			<i>0.0014</i>	<i>0.0016</i>						
3049		1.67	8.50	8.30	2.61					
		<i>0.0008</i>	<i>0.0028</i>	<i>0.0028</i>	<i>0.0015</i>					
2953		3.87	9.10	9.29	5.29	-0.10				
		<i>0.0018</i>	<i>0.0025</i>	<i>0.0025</i>	<i>0.0025</i>	<i>0.0007</i>				
2858	-0.76	5.73	8.41	7.72	7.99	1.77				
	<i>0.0003</i>	<i>0.0020</i>	<i>0.0020</i>	<i>0.0022</i>	<i>0.0024</i>	<i>0.0014</i>				
2763	-0.02	7.21	8.31	5.97	7.58	4.23	-2.03			
	<i>0.0004</i>	<i>0.0017</i>	<i>0.0015</i>	<i>0.0017</i>	<i>0.0019</i>	<i>0.0018</i>	<i>0.0002</i>			
2668	1.36	7.93	7.56	4.87	5.43	5.20	-0.80			
	<i>0.0005</i>	<i>0.0012</i>	<i>0.0012</i>	<i>0.0011</i>	<i>0.0015</i>	<i>0.0016</i>	<i>0.0006</i>			
2572	3.19	7.28	6.72	4.26	3.67	4.37	-0.003			
	<i>0.0008</i>	<i>0.0010</i>	<i>0.0009</i>	<i>0.0006</i>	<i>0.0010</i>	<i>0.0011</i>	<i>0.0007</i>			
2477	3.63	6.50	6.49		2.83	2.76	0.76			
	<i>0.0010</i>	<i>0.0009</i>	<i>0.0005</i>		<i>0.0003</i>	<i>0.0004</i>	<i>0.0003</i>			
2382	2.41	5.47	6.11				2.68			
	<i>0.0010</i>	<i>0.0011</i>	<i>0.0007</i>				<i>0.0003</i>			
2287	1.13	4.37	6.17	2.80		4.98	6.40	3.03	1.23	
	<i>0.0008</i>	<i>0.0011</i>	<i>0.0012</i>	<i>0.0002</i>		<i>0.0008</i>	<i>0.0011</i>	<i>0.0006</i>	<i>0.0002</i>	
2192	-1.27	1.66	4.59	4.43	2.60	5.94	7.77	6.91	5.43	
	<i>0.0003</i>	<i>0.0004</i>	<i>0.0010</i>	<i>0.0011</i>	<i>0.0004</i>	<i>0.0013</i>	<i>0.0011</i>	<i>0.0012</i>	<i>0.0012</i>	
2096			2.18	4.42	5.42	7.31	7.25	6.94	6.13	
			<i>0.0007</i>	<i>0.0010</i>	<i>0.0010</i>	<i>0.0009</i>	<i>0.0011</i>	<i>0.0010</i>	<i>0.0010</i>	

Vertical velocity in m s^{-1} ; cloud water mixing ratio in kg kg^{-1} (in italics, below).

Vertical slice through simulated cloud showing cloud droplet spectra at each grid point, resolution = 95 m. $N_0 = 1000 \text{ cm}^{-3}$.

Corresponding *cloud mixing ratios* and vertical velocities. The aircraft penetration was at $\sim 2700\text{m}$.

It can be seen in Fig. 4 that the model predicts that the number of drops larger than 25μ , and the size of the largest drop increases with height in the diluted updraught at $x = -0.6$ km (Fig. 5, 48 min). The updraught is the centre part of the thermal circulation and contains a mixture of cloud base air and environmental air. Table 1 shows that the values of $L/L_{ad} \sim 0.6$ while the updraught speed was about 9 m s^{-1} ; ideal conditions for enhanced growth due to entrainment and mixing (Baker et al, 1980). The observations suggest that although the number concentration is likely to be constant in the updraught due to re-activation of CCN, the larger drops compete more effectively for the water vapour and growth of these drops is favoured (Baker et al, 1980).

10th August 1995 SCCMS case study, of “maritime”
type.

Radar scan, 10th August 1995

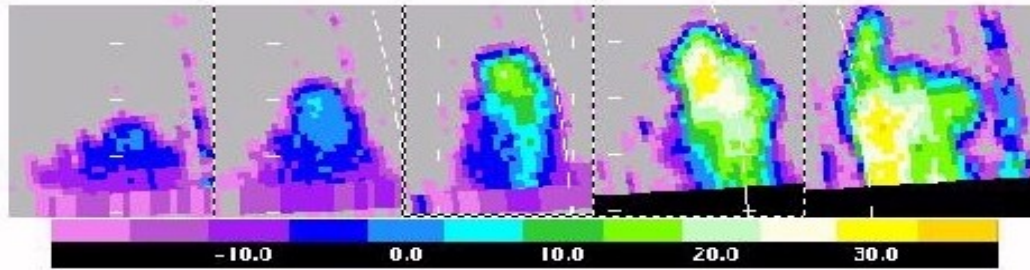


Fig 3: Five vertical scans through cloud at (left to right) 1456:00, 1458:15, 1500:30, 1502:27 and 1506:39. Horizontal and vertical scales are 1 km and 2 km respectively with the lowest tick marks at 1 km.

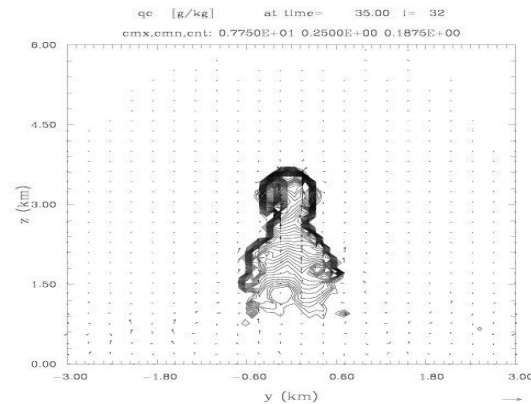
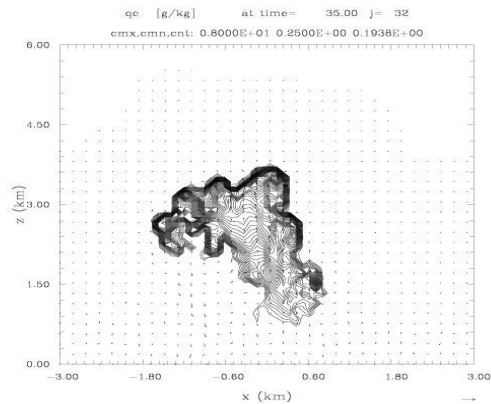


Fig 4: x-z plot (left) and y-z plot (right) of cloud water produced by model in centre of domain.

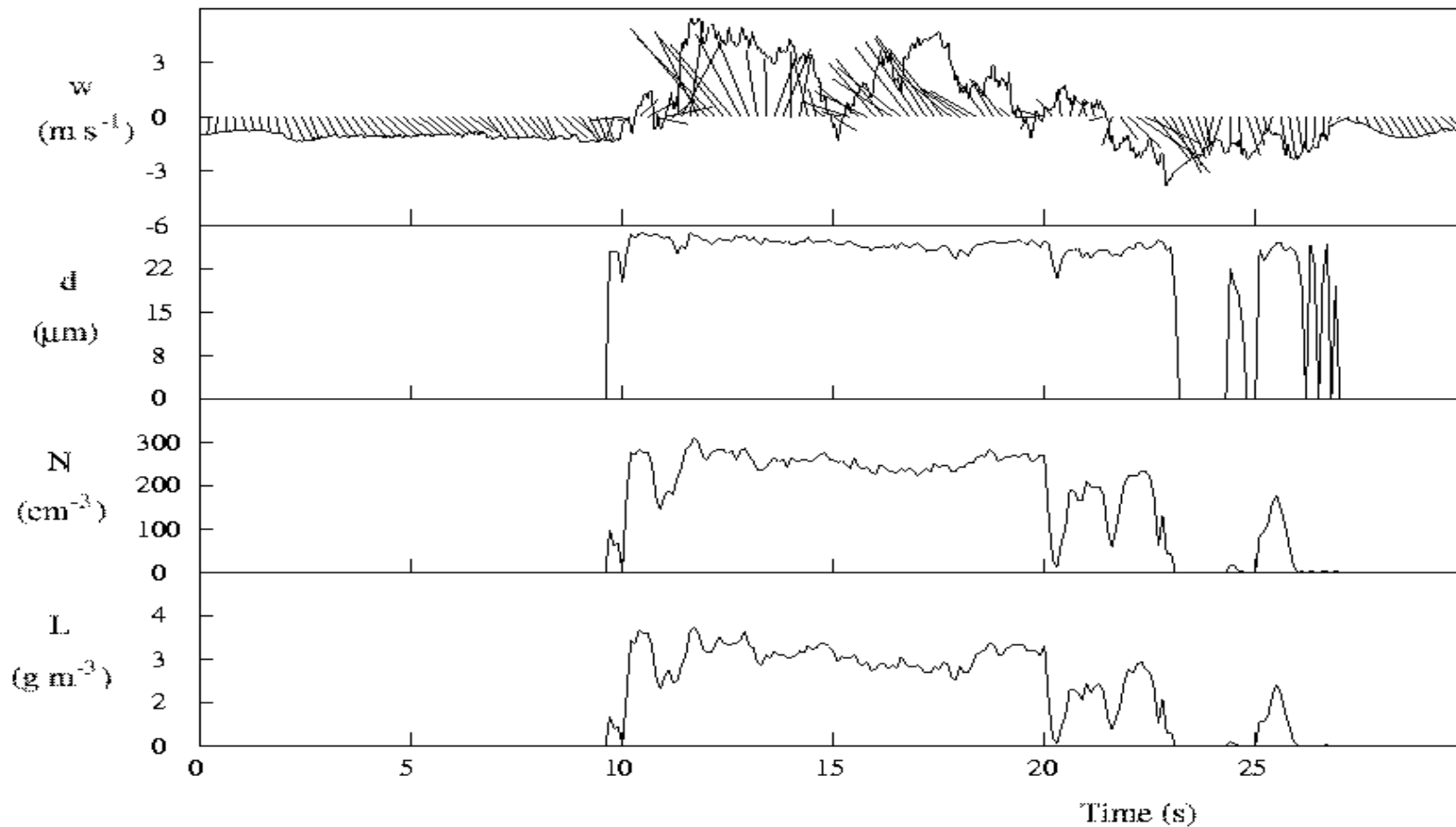


Fig 8. Time series of data gathered beginning at 1726:40. The top panel shows the 25 Hz vertical wind speed (w) superimposed with wind vectors calculated from the vertical wind and horizontal wind along the direction of motion; the bottom three panels are 10 Hz values of mean diameter, total concentration of cloud drops N , and liquid water content, L , respectively, derived from the FSSP.

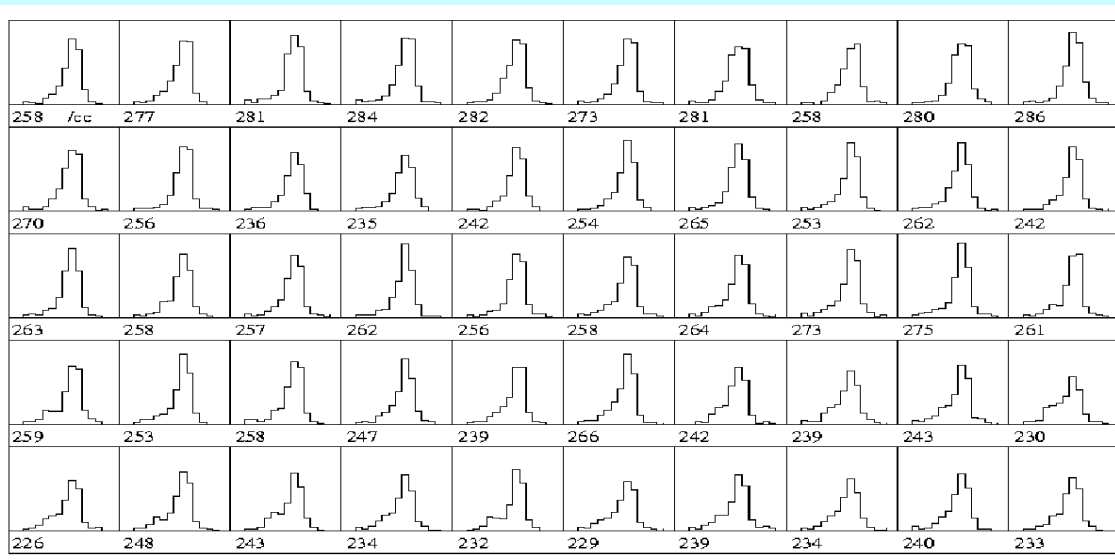


Fig 9. 10 Hz drop size distributions measured by the FSSP commencing at 1726:52 (top left) and ending at 1732:20 (bottom right). The x-axis is diameter ranging from 0 - 50 μm and the y-axis is $N(d)$, ranging from 0 - 100 cm^{-3} .

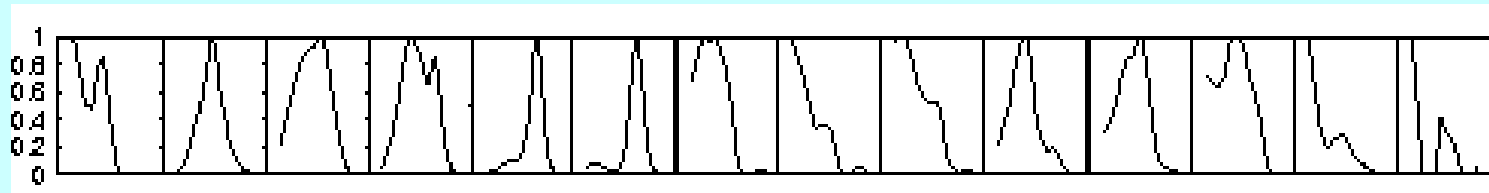


Fig 10. Simulated drop size distributions through cloud along flight path (altitude 2.4 km), ($N_0=500 \text{ cm}^{-3}$). Each plot represents a grid point in the model (95 m), and corresponds to approximately 1 second of flight time, from top left to bottom right. The x-axis is diameter ranging from 0--40 microns and the y-axis is the normalized distribution.

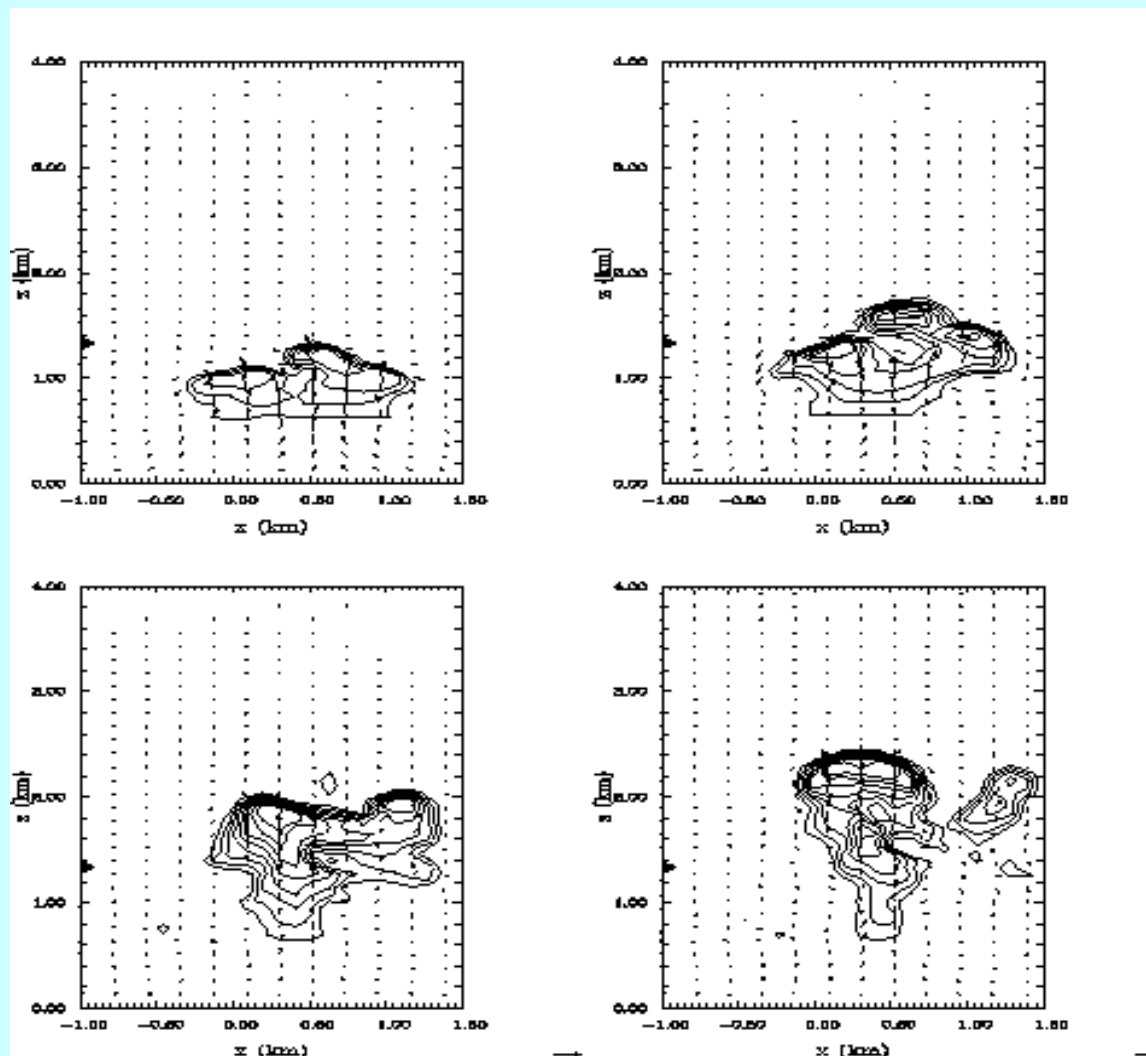


Fig 11 Vertical cross-sections of simulated cloud water mixing ratio with wind vectors overlaid at (top left) 65, (top right) 68, (bottom left) 71, and (bottom right) 73 minutes.

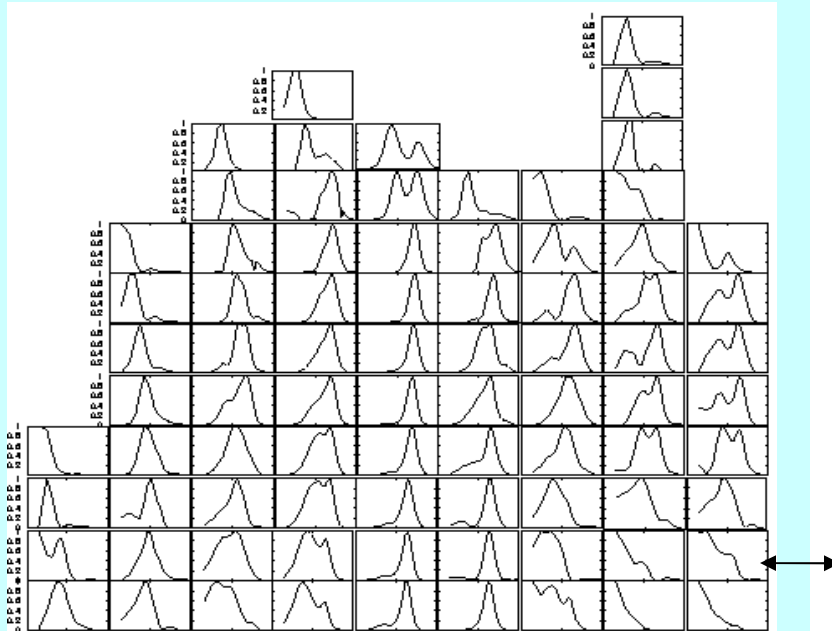


TABLE 2. 10TH AUGUST 1995: SIMULATED VERTICAL VELOCITIES AND CLOUD WATER MIXING RATIOS FOR THE UPPER REGION OF THE CLOUD AT 71 MINUTES.

Height (m)	Distance from edge of cloud (m)								
	0	95	190	285	380	475	570	665	760
3240									-0.59 <i>0.0008</i>
3144				2.27 <i>0.0004</i>					-1.35 <i>0.0005</i>
3049			1.29 <i>0.0009</i>	7.11 <i>0.0022</i>	4.04 <i>0.0010</i>				-2.06 <i>0.0001</i>
2953			2.98 <i>0.0022</i>	10.76 <i>0.0039</i>	9.63 <i>0.0037</i>	4.45 <i>0.0019</i>	-0.94 <i>0.0007</i>		-2.23 <i>0.0006</i>
2858	-1.44 <i>0.0005</i>	4.99 <i>0.0028</i>	11.79 <i>0.0041</i>	13.55 <i>0.0040</i>	10.88 <i>0.0040</i>	13.6 <i>0.0020</i>	-1.42 <i>0.0015</i>		-2.25 <i>0.0010</i>
2763	-1.5 <i>0.0008</i>	6.73 <i>0.0027</i>	12.69 <i>0.0035</i>	13.54 <i>0.0040</i>	13.39 <i>0.0037</i>	6.44 <i>0.0032</i>	0.14 <i>0.0025</i>	0.31 <i>0.0025</i>	0.19 <i>0.0023</i>
2668	-0.53 <i>0.0011</i>	7.80 <i>0.0027</i>	12.84 <i>0.0033</i>	13.81 <i>0.0037</i>	11.43 <i>0.0030</i>	9.26 <i>0.0031</i>	3.0 <i>0.0027</i>	0.19 <i>0.0020</i>	0.19 <i>0.0020</i>
2572	1.11 <i>0.0015</i>	8.77 <i>0.0027</i>	11.65 <i>0.0031</i>	14.26 <i>0.0034</i>	11.53 <i>0.0028</i>	8.46 <i>0.0028</i>	4.94 <i>0.0026</i>	3.15 <i>0.0023</i>	3.15 <i>0.0023</i>
2477	-2.46 <i>0.0003</i>	3.67 <i>0.0015</i>	8.62 <i>0.0023</i>	10.76 <i>0.0026</i>	14.06 <i>0.0033</i>	12.24 <i>0.0029</i>	8.0 <i>0.0022</i>	6.02 <i>0.0024</i>	4.65 <i>0.0023</i>
2382	-1.20 <i>0.0003</i>	4.20 <i>0.0014</i>	7.58 <i>0.0019</i>	9.57 <i>0.0023</i>	13.00 <i>0.0031</i>	11.83 <i>0.0029</i>	7.04 <i>0.0013</i>	5.14 <i>0.0016</i>	4.82 <i>0.0016</i>
2287	-1.0 <i>0.0005</i>	5.72 <i>0.0015</i>	6.12 <i>0.0017</i>	8.06 <i>0.0020</i>	11.52 <i>0.0028</i>	11.12 <i>0.0029</i>	6.17 <i>0.0007</i>	2.91 <i>0.0008</i>	3.27 <i>0.0010</i>
2192	2.57 <i>0.0010</i>	4.81 <i>0.0012</i>	4.21 <i>0.0012</i>	6.62 <i>0.0015</i>	10.15 <i>0.0026</i>	10.75 <i>0.0028</i>	5.79 <i>0.0013</i>	1.48 <i>0.0003</i>	2.7 <i>0.0006</i>
2096	2.15 <i>0.0004</i>	3.55 <i>0.0007</i>	2.81 <i>0.0007</i>	5.35 <i>0.0012</i>	9.07 <i>0.0024</i>	9.71 <i>0.0026</i>	5.91 <i>0.0025</i>	2.08 <i>0.0007</i>	2.75 <i>0.0005</i>
2001		1.91 <i>0.0002</i>	1.48 <i>0.0002</i>	4.31 <i>0.0011</i>	7.92 <i>0.0022</i>	8.47 <i>0.0025</i>	5.65 <i>0.0024</i>	3.19 <i>0.0018</i>	1.98 <i>0.0011</i>

Vertical velocity in m s^{-1} ; cloud water mixing ratio in kg kg^{-1} (in italics, below).

Vertical slice through simulated cloud showing cloud droplet spectra at each grid point (resolution 95 m). $N_0=500 \text{ cm}^{-3}$.

Corresponding *cloud mixing ratios* and vertical velocities. The aircraft penetration was at $\sim 2400\text{m}$.

There are explicit differences between the two cases.

The 10/8/95 study, more typical of a maritime environment, with a smaller value for N_0 , has narrower observed and modelled spectra with less bimodality. The simulation spectra indicate the effects of the turbulent mixing and entrainment processes at the top, sides and around the “holes”; observable near the top of the cloud.

A grid resolution of 95m. is too large to properly resolve the entrainment. It is hope to repeat the studies with a 20m resolution. There is evidence of the broadening of the spectra in the updraft after entrainment has occurred, and with modelling sensitivity studies, bimodality decreased with increasing N_0 (to be published).

Summary

24th July case (continental):

- model predicts the number of drops larger than 25 microns, and shows that the size of the largest drop increases with height in the diluted updraught at $x = -0.6$ km (Fig. 3, 48 min).
- updraught is the centre part of the thermal circulation and contains a mixture of cloud base air and environmental air. Table 1 shows values of $L/L_{ad} \sim 0.6$ and $w \sim 9$ m s⁻¹; ideal conditions for enhanced growth due to entrainment and mixing (Baker et al, 1980).
- observations suggest that although the number concentration is likely constant in the updraught due to re-activation of CCN, the larger drops compete more effectively for the water vapour, and growth of these drops is favoured (Baker et al, 1980).

10th August case (maritime):

- observed and modelled spectra both indicate less bimodality and are narrower than the 24th July case
- simulation spectra indicate the effects of the turbulent mixing and entrainment processes at the top, sides, and around the “holes” – in this case only observable near the top of the cloud.
- evidence of broadening of spectra in updraught after entrainment occurs. Sensitivity studies show bimodality decreases with increasing N_0 (to be published).

.....and Questions?

Is the data representative?

Why is the continental case more bimodal than the maritime case?

What are the entrainment turbulent mixing processes?

Does this evidence of broadening near the 'holes' occur after entrainment?

Does the maritime case 10/8/95 produce larger sizes more quickly?

Does a decrease in N_0 mean an increase in bimodality?

The differences in these two clouds droplet spectra shows a significant difference in the bimodality, which will effect the generation of larger droplets which generate coalescence.

